

Improving the Resolution of the Cylindrical Mirror Analyzer (CMA) by Segmentation

David Edwards Jr., *Member, IAENG*

Abstract— The standard cylindrical mirror analyzer (CMA) has been modified by dividing the inner and outer electrodes into segments and setting the voltages on these segments to obtain the best value for the energy resolution. It has been found that dividing both the inner and outer electrodes into only one segment has resulted in an energy resolution of 0.017% for entrance angles of 42.3± 6 degrees. This corresponds to more than an order of magnitude improvement in the resolution over that of the standard instrument when operated at the minimum trace width point.

Index Terms—CMA, cylindrical mirror analyzer, energy analyzer, spectrometer.

I. INTRODUCTION

A. A brief history of the CMA

The first mention in the literature of the cylindrical mirror analyzer was apparently by Blauth (1957) [1] who reported the CMA being used in experimental work. A careful analysis of the CMA was ~10 years later given by Zashkvara et al [2] and Sarel [3] who found that for the special angle of 42.3 degrees the order of the focus would become 2 resulting in a significant reduction in the effective spot size from those CMA devices operating at other angles. A further development came shortly after in a paper by Hafner, Simson and Kuyatt [3] in which they noted that the spot size for an order 2 device occurs slightly before the axis crossing and has a width reduced by a factor of ~4 from its axis value. Thus in ~1967 the instrument known as the cylindrical mirror analyzer was defined while two years later Palmberg, Bohn, and Tracy [4] reported its first implementation an instrument called the Auger electron spectrometer which has come into widespread in surface analysis instrumentation.

Thus the cylindrical mirror analyzer (CMA) has become one of the 3 most widely used electron spectrometers currently employed in scientific instrumentation. Given its ubiquitous presence it is surprising that little improvement in its resolution has been found in the ~40 years since its inception.

It is the purpose of this report to describe such an improvement effected by the rather simple expedient of electrode segmentation.

II. THE MODELING

A. Some notation

Particles will be considered to start out from a point on the axis making an angle of $\alpha_0 \pm \alpha_{\max}$ with respect to the axis. The set of angles between the extremes will be denoted as a bundle. Each ray in this bundle after passing through the spectrometer will intersect the axis at a position denoted by z_i and the extent of the set z intercepts will be denoted by spot size. I.e. it is the size of the extents of the intercepts of the trajectory bundle. Thus even though the particles emanate from a single point on the axis upon re reaching the axis they will have spread into this finite interval denoted by spot size.

The bundle size used in this study is 6 degrees, this having become somewhat standard in a listing of the properties of electron spectrometers.

B. The geometry

The CMA itself is an idealized device having the potential appropriate to cylindrical electrodes of infinite extent. However to model such a geometry the end locations must be truncated to finite positional values. As this work does not wish to be concerned with the effect of such a truncation the end plates of the cylinders are positioned sufficiently far from the trajectory region to make their influence negligible and hence the unsegmented model was designed so that it may approximate that of the ideal CMA.

The segmentation of the device is effected by dividing both the inner and outer cylinders into n equal length segments. This construction is shown in figure 1 for a 3 segment division and further defines the nomenclature of the various elements of the device.

In this figure are also shown segments preceding the first segment (presegment) and the segment following the last one (postsegment). It is noted that the start (end) positions for outer segments were made so there was some overlap with the inner segments. The geometry itself while being cylindrically symmetric has an additional symmetry about $z=0$.

The bundle size being 6 degrees the starting point of the first inner segment was located at the intersection point of a 10 degree ray rather than for a 6 degree ray thus ensuring that the maximum ray in the 6 degree bundle will be further from the discontinuity present at the junction of the inner presegment and the first inner segment than it would have been were the starting point set using the 6 degree ray.

It is noted that all of the labeled lines in figure 1 have voltages that may be adjusted in order to find the optimum solution (the minimal spot size). The exception to the above

Manuscript received December 20, 2015.

David Edwards Jr. is with the IJL Research Center USA phone: 802-274-5845; e-mail: dej122842@gmail.com

is that the inner pre and post segments were fixed at 0 thus avoiding refraction effects at the inner cylinder interface. It is further considered that the potential is 0 everywhere below the inner cylinder implying that the trajectories from the starting point to the inner cylinder and from the inner cylinder to the ending point were in a field free region.

The radii of the inner and outer electrodes are denoted by R_{in} , R_{out} while the starting position on the z axis is given by $-s_i$. The defining parameters of the geometry are given in the following table.

Table 1: the geometric parameters (dimensionless) of the modeled CMA.

Rin	37	Rout	80
left end plate	-187	right end plate	187
inner segments start	-54.47	inner segments end	54.47
outer segments start	-70	outer segments end	70
start position	-113	alpha0	42.3 deg
bundle	6 degrees		

The total segment length is given by the difference between segment end and segment start. This length divided by the number of segments yields the segment length particular to each cylinder. It is perhaps worthwhile to remark that the parameters found are all user selectable and once having been chosen are independent of the number of segments used in the device segmentation.

B. Potential modeling

The determination of the trajectory of a particular ray requires the knowledge of the electric field at every point in its travel which in turn requires the potential be known at all points between the two cylinders. The potentials have been determined via a high precision FDM process [5] and for the purposes of potential determination an order 10 algorithm has been used. The mesh point overlay for the specific geometry is given at all integral points in figure 1. The potentials near the junction of segments with dissimilar potentials are of course singular and result generally in large errors that propagate throughout the mesh. The effect of these singularities has been mitigated by the use of a set of 10 telescoping child regions converging on the singular point itself [6]. The dimension of each child region has been taken to have a height equal to its width equal to 20 (in units of the parent mesh). As will be later seen in the verify section this construction has been found sufficient to effect precisions consistent with the spot size itself. A more complete elaboration of the potential calculations and singularity neutralization can be found in references [5, 6].

C. Trajectory modeling

The ray starts out from a position of $-s_i$ on the z axis making an angle α with respect to the axis. The initial part of its travel is in a field free region and hence is

undeflected till it crosses the inner cylinder boundary. After crossing this boundary it travels along a path determined by the electric field at points on its trajectory. This calculation itself has been made using a recently developed ray trace process [7] allowing for independent settings of the order of the space and time algorithms (see reference [7] for both a definition of terms and description of the process). Here it is simply noted that the time order was taken to be 10 in all situations while the space order was taken typically to be of order 4. Again the precision of the 4th order algorithm in the ray trace process was found sufficient consistent with the resultant spot size of the optimal solution. Also it is remarked as has already been stated that the potential calculations themselves were done with the order 10 algorithm. It is only in the ray trace where interpolations for the electric field at a point on the trajectory that the order 4 algorithm was utilized as its execution time was in some cases considerably shorter than the higher order algorithms and the trajectories themselves did not suffer from its slight lack of precision.

D. Finding the minimal spot size

The bundle of rays starting their trajectories from the point $-s_i$ on the z axis (see figure 1) contain all rays with angles within the bounds of the bundle. Further all rays have the same kinetic energy E_0 . This set of rays when intercepting the axis at the end of their trajectories do not intercept the axis at a single point but in a distribution of intercept points the width of which is defined as the spot size. Since to lowest order the energy resolution of the instrument is proportional to the spot size of the exiting rays, finding the optimum resolution is equivalent to finding the minimum spot size. Thus since the spot size itself is dependent on the voltages placed on the segments prior to the trajectory calculations, one can look for the set of voltages that yields the minimum spot size and thus obtain the optimum resolution for the device. This set of voltages is considered as coordinates of the optimal operating point. The procedure for finding the optimal operating point is next described.

E. Finding the optimal operating point

The process for finding an optimal operating point will be described for a generalized spectrometer that consists of an outer electrode, an inner electrode, and possible end terminations. It is assumed without loss of generality that there is some set of voltages that exist on the individual elements. The voltages on the elements are adjusted till a low order focal point is found on the exit plane (in our case the z axis). The geometry is then divided in some manner into n segments and the voltages of these segments are set to the voltages used to obtain the previous low order focal point. This set is then optimized with an optimization algorithm using small steps (for one possible algorithm, see the discussion below). This resultant solution is then considered to be and denoted by the "primary solution", and will typically only slightly improve (less than a factor of 2) the resolution of the device from its unsegmented value.

Now after finding the primary solution a solution which will be referred to and denoted by the "secondary solution" will be sought, the "secondary solution" being any solution with spot size reduction from the primary solution $> \sim 3-5$. Finding such a solution has been accomplished in the present work with the aid of the following algorithm. The

first step of the algorithm is to choose a new operation point that should be significantly distinct from that of the primary solution so that that a “small step optimization” would likely not bring the solution point back to the primary point. The selection of the starting operating point is typically a trial and error process and depends in a large measure on the user’s observation and experience gained over a number of trials.

However, although little insight can be offered in choosing the initial starting point, the following process has been found very useful in finding a minimum spot size from a given initial point.

F. The optimization process

The values of the segment voltages can be considered as the coordinates of a hyper point in an n dimensional hyperspace.

From the coordinates of the hyperspace a list of the parameters of the space is formed and a hyper point chosen. The parameter list is then scanned with a small step algorithm, described below, and at its completion a minimum spot size has been found and a global minimum set to this value.

Thus at this point one has both a hyper point and a value of the spot size corresponding to this point. Two loops, an outer and an inner, are then formed. When scanning the outer loop an element in the parameter list is chosen and its value is incremented first incremented and later decremented by a fixed step (~1.0).

For each outer loop value, the parameter list is again scanned in an inner loop with a smaller step (~.1) and with a slightly different algorithm. The algorithm consists in the following: For each parameter in inner scan its value is first incremented and then decremented. If either produce a spot size less than the current minimum the current minimum reset and a new value obtained with the step in the same direction. When no further reduction in the spot size is found the small step reduced by a factor of 10 and the process repeated. The repetitive scan of the inner loop is terminated when the inner loop step becomes less than a user selectable value. At this point the next value in the outer loop is chosen and the process repeated. The process is continued until the outer loop scan is completed.

At this point the process is restarted with however a reverse scan made through the parameter list.

If at the end of the above the current minimum has changed from its value at the start a new double scan is initiated.

When no further reduction of the current minimum value has been found it has been found useful to randomly mutate the coordinates of the minimum hyper point and commence again the double loop process. When no significant further reduction in the value of the minimum spot size has been found, the process terminates.

The advantage of the above is that very little user intervention is required, other than initially setting a trial hyper point. The disadvantage is the time involved from the initial starting point to the time at which it becomes clear than no further random mutation of the optimal hyper point would give a significant reduction to the minimal spot size is lengthy. It can be several 24 hour periods.

G. The standard CMA

As comparisons will be made of the results of the segmented CMA, to the standard CMA, the standard CMA will be modeled here by setting all outer segment voltages to their theoretical value while all inner voltages are set to 0.

The standard CMA geometry of our model has Rin = 37, Rout = 80, and E0 is given by:

$$E0 = 13.098 / \text{Log} (\text{Rout} / \text{Rin}) [2, 3].$$

The following tabulates the results obtained by the present calculations and those from [4] and/or [9] all a 6 degree bundle.

Table 2. A comparison with the present results with those of references [4] and [9].

	references [4] or [9]	present
spot size (on axis) E0 16.9859	1.3086 [4]	1.3277
min trace width (slightly above axis)	0.32715 [4] reduction 4.0 reduction ~3 [9]	.396(graphical) reduction 3.35
spot size (after minimization)	-----	.34781 reduction 3.82 (E0 17.2039)
delta E/E0	.2% from min trace width [9]	.203% E0 17.2039 from minimization wrt E0
rc	3.07	2.15

This table shows a general agreement of the present results with the previous data of HKS[4] as well as that reported in [9]. It also gives the results of minimizing the on axis spot size with respect to a variation of E0. Seen is that in effect the minimization moves the minimum trace width from its position slightly above the axis onto the axis with a slight diminution of its value. It is noted that this effect is also seen in figure 2-14 of reference [9] in which for an increase in energy of 1% the min trace width moves close to but is still above the axis. It is puzzling as to why this simplification of the standard geometry had not been previously reported since the phenomena was clearly apparent in the figure of ref [9]. Such a simplification would have replaced the construction of an annular slot at an off axis position by a more easily constructed annular aperture. Finally a location of the minimum trace width (rc) is reported at a markedly different position from that of [4] which could not be accounted for either by either significantly degrading the present modeling precision or by any reasonable change in the end plate voltages. If the current modeling is correct this would imply a slight change in the ratio of rc/r1 where r1 is the inner cylinder radius in table 1 of [4] from .083 to .058. It is noted that such a discrepancy would only affect the resolution by ~20-30%, a measureable but not significant effect.

H. The segmented CMA

Geometries were constructed having a number of segmentations. Each segmentation required a rather lengthy process, as described above, to obtain the minimum spot size for that segmentation. It is of course clear that it is not known whether either the global minimum was found or if a considerable reduction might even yet be obtained with another set of parameters. The values reported were simply the smallest values obtained in the present study.

1) Optimizing the outer and inner segments

Results of the dependence of spot size on the number of segmentations are shown in figure 2. It is noted that the reduction for a particular segmentation is compared to the

spot size of the standard CMA after the minimization wrt E_0 and not the full trace width of the standard CMA. Seen in figure 2 are results for both a variation of both the inner and outer values and those for fixing the inner segments values at 0 and adjusting only the outer segment values. Number of segments = 0 refers to the standard CMA discussed above. There are several notable features evident in this figure. The first surprising and in fact unexpected finding is that a one segment segmentation has given results quite similar to the other segmentations. The second is that allowing a variation in both the outer and inner parameters gave significantly enhanced spot size reductions when compared with varying the outer only parameters. That being said it is clear that the outer only curve is able to obtain a spot size reduction of ~ 4 itself noteworthy. It should be noted that as mentioned above determining the minimum spot size for a given set of parameter was lengthy and was equally so for the data points in outer only curve. Said slightly differently one obtains the factor of 4 reduction using the outer only segments by the lengthy search for the "second solution" in a manner described above. And lastly when considering one segment only the values of both the outer and inner segments must be included in the optimization to obtain an appreciable reduction factor.

2) *One segment segmentation*

As remarked above the results of one segment segmentation were essentially the same as any higher segmentation and so this will be the construction whose properties will be reported. The following table gives the optimized parameters as well as the resultant minimum spot size and intercept of the centroid of the bundle on the z axis. It should be noted that the values of both end plates were fixed at 10. The spot size represented the extent of the intercepts of the 6 degree bundle with angular spacing of $\frac{1}{2}$ degree.

Table 3. The optimized parameters for the 1 segment construction.

inner presegment	0	outer presegment	20.213
inner v1	-2.557	outer v1	9.068
inner postsegment	0	outer postsegment	13.844
E_0	19.8859	z intercept	124.85
minimum spot size	.026929		

3) *The resolution of the single segment segmentation*

The resolution is measured by finding the set of intercept points for energies E_0 , $E_0(1+x)$, $E_0(1-x)$ and then determining the smallest x such that the sets are disjoint. This can be easily understood from figure 3 in which rays in the bundles having 3 separate energies are plotted.

Seen is that the intercepts for each of the distributions are clearly disjoint implying that the energy resolution is less than 0.05%. The minimum value of x has been found to be .017% consistent with figure 3. It should be noted that within the bundles, 25 equispaced values between 6 and -6 were used. As the resolution for the standard CMA after minimization wrt E_0 has been found to be .203 % (see

above) a resolution improvement of ~ 12 has been obtained. This is also consistent with the spot size reduction factor of ~ 13 seen in figure 2 for the one segment construction.

4) *Verification*

A test of the validity of the one segment results (minimum spot size, z intercept) was made by scaling the geometry by a factor of 2. Since precisions are for the high order algorithms used in both the potential and ray trace calculations expected to be super linear with respect to this scaling the level of consistency can be obtained from a comparison of the two results.

The following table gives the minimum spot size and the z intercept for the scaled and unscaled geometry. It is noted that all values in the scaled geometry are divided by 2 removing the scale factor from the result.

Table 4. A listing of the spot size and z intercept for various space orders for two meshes.

space order	Δw 37,80	Δw 74,160	zi 37,80	zi 74,160
2	.039486	.0268530	124.815351	124.846238
4	.026929	.0269245	124.856345	124.856376
6	.026920	.0269250	124.856317	124.856396
8	.026920	.0269250	124.856315	124.856396
10	.026920	.0269250	124.856315	124.856396

The above table provides a certain verification of the results to the precisions levels indicated. Seen is that for orders 4 to 10 the spot size and z intercept is independent of the factor of 2 scaling and in fact the order 2 results while differing from the convergent values in the low density mesh provide reasonable estimates of both the spot size and z intercept when used in the higher density mesh.

III. NOTES OF CAUTION

The device which has been modeled clearly does not correspond to a real spectrometer for at least 3 reasons:

- 1 The segments are contiguous, namely there are no inter segment gaps. Such an arrangement would be inappropriate for any real device as small gaps are required to prevent voltage breakdown, the size of the gaps dependent of the voltages involved in the particular application. It is felt if the gaps are small the parameters in table 1 would either give an approximate setting of the optimized voltages involved or would provide a starting operating point from which the optimal values may be found by using a small step optimization algorithm.
- 2 A point source is assumed. The effect of any finite source size would again necessitate remodeling of the device and is again dependent on the particular application.
- 3 The entrance geometry is likely to be unrealistic considering the space and geometry requirements of the total instrument it is to be a part of. In this case the segmentation process described above could be of use in the modeling the device with the necessary entrance geometry.

IV. SUMMARY

A study of the effect of segmentation on the properties of the cylindrical mirror analyzer has been made. Segmentations of between 1 and 5 segments have been

modeled with the somewhat surprising result that the spot size reduction has been found to be relatively independent of the number of segments involved. Further that this reduction for the single segment device has resulted in an energy resolution of 0.017% a factor of ~12 improvement over the standard CMA [4] (when operating at the minimum trace width point).

Segmentation may be of course be useful in other types of devices, namely the 127 degree analyzer (CDA), the 90 degree spherical sector analyzer (SDA) and others [9]. It could also permit these devices to be designed with construction angles suited to the application rather than the

application adapt to the required construction angles as is the current situation. It is also noted that electrode shapes markedly differing from their classical values might be employed themselves being modified by segmentation.

These results suggest that segmentation may in fact represent a new paradigm for the design of electron spectrometers.

Newark, Vermont
December 20, 2015

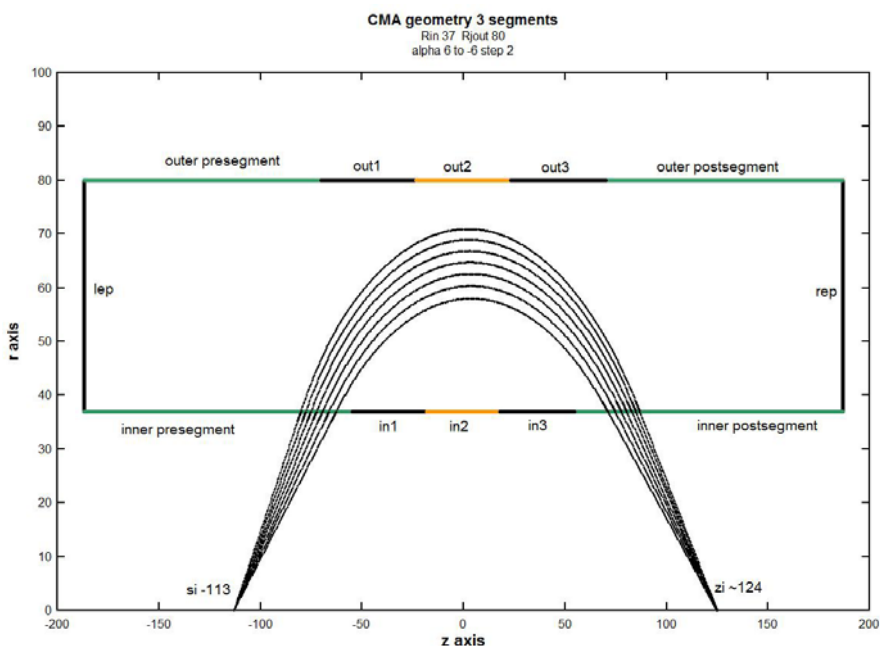


FIGURE 1. SHOWN IS A CMA GEOMETRY HAVING THE INNER AND OUTER CYLINDERS PARTITIONED BY 3 SEGMENTS. ALSO DRAWN ARE THE TRAJECTORIES IN THE 6 DEGREE BUNDLE WITH 2 DEGREE INCREMENTS.

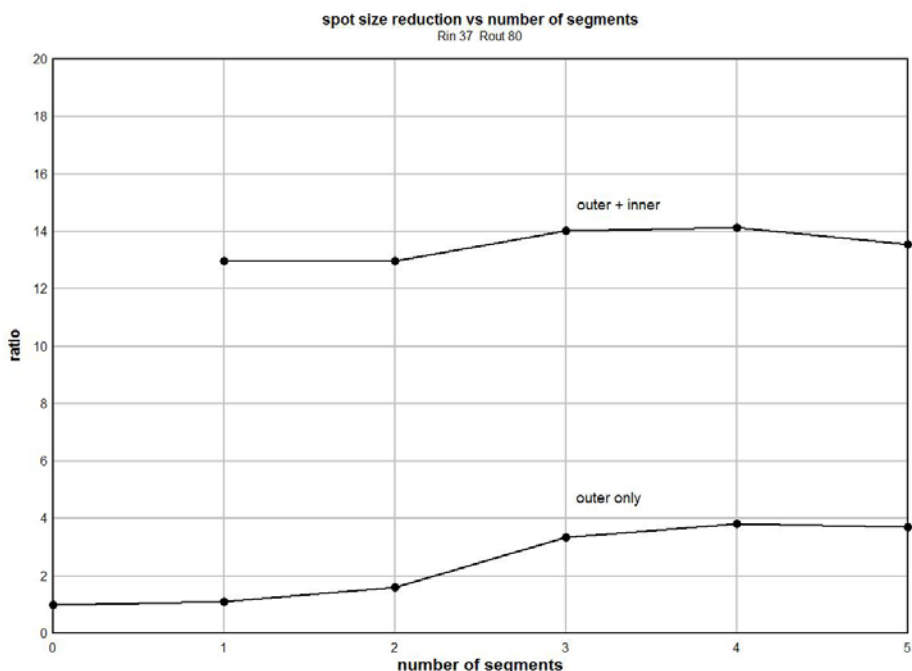


Figure 2. The spot size reduction is plotted as a function of the number of segments used.

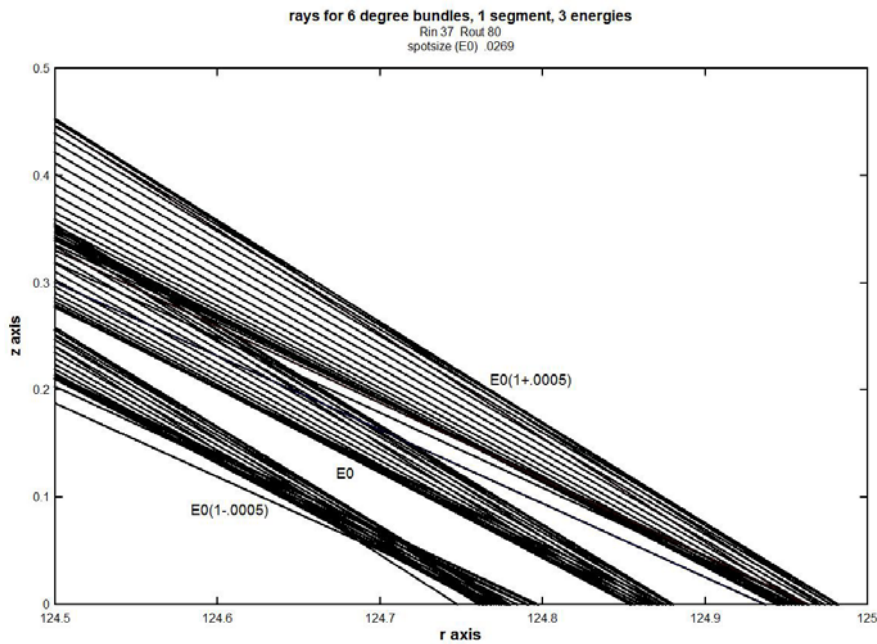


Figure 3. Rays in 6 degree bundles are plotted for 3 separate energies.

REFERENCES

- [1] E. Blauth, Z. Physik 147,228(1951).
- [2] V. V. Zashkvara, M. I. Korsunskii, O. S. Kosmachev, Soviet Phys.-Tech. Phys (English Transl.) 11, 96 (1966).
- [3] H. Z. Sar-el, Rev. Sci. Instr. Vol 38, number 9 (1967) pg. 1210.
- [4] Hafner, J. Arol Simson, and C. E. Kuyatt, Rev. Sci. Instr. Vol 39, number 1 (1968) pg. 33.
- [5] P. W. Palmberg, G. K. Bohn, J. C. Tracy, Applied Physics Letters, Vol 15, number 8 (1969) pg. 254.
- [6] David Edwards Jr, "FDM for curved geometries in electrostatics II: the minimal algorithm." Proceedings of the International Multi Conference of Engineers and Computer Scientists 2014, Vol I, IMECS 2014 March 12 - 14, 2014, Hong Kong
- [7] David Edwards Jr, "Finite Difference Method for Boundary Value Problems. Application: High Precision Electrostatics, Proceedings of the International Multi Conference of Engineers and Computer Scientists 2014, Vol I, IMECS 2014, March 18 - 20, 2015, Hong Kong
- [8] David Edwards Jr, "HIGH PRECISION RAY TRACING IN CYLINDRICALLY SYMMETRIC ELECTROSTATICS" J. Electron Spectroscopy and Related Phenomena, (to be published).
- [9] Anjam Khursheed, Scanning Electron Microscope Optics and Spectrometers, World Scientific Publishing Co. Ptc. Ltd., ISBN -13 978-981-283-667-0 pg. 99.